ADJACENCY-BLURRING-EFFECT OF SCENES MODELED BY THE RADIOSITY METHOD

C.C. Borel and S.A.W. Gerstl
Space Science & Technology, SST-8, MS D438
Los Alamos National Laboratory
Los Alamos, New Mexico 87545, USA

Abstract

In this paper we describe a method to simulate images through a scattering atmosphere. We compute the scattering of light from adjacent surfaces into the field-of-view (FOV) with the extended radiosity method. Our simulation takes aerosol scattering phase functions and ground bidirectional reflectance distributions (BRDF) into account.

1 Introduction

The adjacency-blurring-effect is observed at the boundary between a dark and a bright surface. Near the edge over a dark surface photons from the nearby bright surface may be scattered within the atmosphere into the field of view (FOV) of an airborne or satellite sensor. Conversely, near the edge over a bright surface fewer photons reach the sensor's FOV. At a sharp discontinuity in the surface reflectance the intensity transect appears as a sigmaoid instead of a step function.

The adjacency-blurring-effect may introduce errors in the detection and classification of small bright targets surrounded by a dark region or dark targets on a bright background. One can model the blurring due to the adjacency effect with a point spread function (PSF). This PSF is a filter function which is convolved with the unperturbed (no atmosphere) reflectance image of a surface. Other researchers of the adjacency effect are : Pearce (1977), Tanré (1981), Kaufman (1984), Diner and Martonchik (1985) and Richter (1990). Most PSF's are generated by Monte Carlo based methods and are assumed to be rotationally symmetric, thus are not valid for off-nadir views. In the situation of an oblique viewing sensor it is necessary to compute off-nadir PSF's which are generally asymmetric.

We introduce a method to compute the point spread function for any view direction and any layered atmosphere which includes scattering phase functions. The method is based on the extended radiosity method, Borel and Gerstl (1991). We then refine the method to non-Lambertian surfaces and show an algorithm to simulate adjacency blurred images which include vegetated, bare soil and water surfaces.

2 Computing the Point Spread Function for Lambertian Surfaces

In an optical system the point spread function $PSF(x, y, z; x_0, y_0, z_0; \theta_s, \phi_s; \theta_r, \phi_r)$ can be defined as the scattering contribution of a surface element $dA = dx\ dy$ illuminated from direction (θ_s, ϕ_s) located at $(x, y, z = z_0)$ into the line-of-sight direction of the observer (θ_r, ϕ_r) looking at point (x_0, y_0, z_0). Figure 1 shows the geometry for the ground to atmosphere scattering. One can show (see Borel and Gerstl (1992)) that the unitless PSF is given by :

$$PSF(x,y,\ldots) \;=\; \frac{\kappa_s\;\Delta l}{4\;\pi}\sum_{k=1}^{K}\frac{\tau(r_k)\;\;\cos\theta_{r,k}\;f(\theta_{p,k})\;dx\;dy}{\pi\;r_k^2}\cdot\exp(-\kappa_t\;(K-k)\;\Delta l), \tag{1}$$

where κ_s is the scattering coefficient in $[m^{-1}]$, $\Delta l = L_z/(K\cos\theta_r)$, L_z is the height of the scattering atmosphere, K is the number of layers in the atmosphere, $\tau(r_k) = \exp(-\kappa_t r_k)$, κ_t is the total scattering coefficient in $[m^{-1}]$, r_k is the distance between surface point $\vec{P}$ and a point $\vec{P_k}$ on the line-of-sight in the k-th layer, $\theta_{r,k}$ the view zenith angle to dA, $f(\theta_{p,k})$ is the scattering phase function of the k-th layer and $\theta_{p,k}$ is the scattering phase angle. Note that this method takes height dependent scattering and absorption coefficients and even height dependent scattering phase functions into account. The method can even be extended to include terrain effects when the PSF is computed for each pixel in the scene. For the Lambertian surface the PSF for nadir view is rotationally symmetric and asymmetric for all non-nadir views.

According to Borel and Gerstl (1992), the measured radiance $I_{measured}(x,y,z;x_0,y_0,z_0;\theta_s,\phi_s;\theta_r,\phi_r)$ in $[W\;m^{-2}]$ at the sensor for a Lambertian surface is given by :

$$I_{measured}(x,y,\ldots) \;=\; \frac{E_0}{\pi}\tau_s\Big[\tau_r\rho(x_0,y_0)\;+\;\rho(x,y)\otimes PSF(x,y,\ldots)\Big]\;+\;I_{path} \tag{2}$$

where E_0 is the direct energy incident from the sun in $[W\;m^{-2}]$, $\tau_s = \exp(-\kappa_t L_z/\cos\theta_s)$, $\tau_r = \exp(-\kappa_t L_z/\cos\theta_r)$, $\rho(x,y)$ is the reflectance at point (x,y), $\otimes$ denotes the convolution and I_{path} is the path radiance or radiance due to scattering in the atmosphere.

3 The Point Spread Function for Non-Lambertian Surfaces

In practical situations the imaged ground surface is non-Lambertian and thus the above described method may lead to inaccurate simulated images. We attempt now to include the bidirectional reflectance distribution function (BRDF) in the computation of the PSF. First, let us assume that the entire surface has the BRDF :

$$f(x,y,z;\theta_s,\phi_s;\theta_r,\phi_r) = f(\theta_s,\phi_s;\theta_r,\phi_r).$$

Second, that the contributions from indirect skylight are negligible on the radiance in direction $(\theta_{r,k},\phi_{r,k})$ or that the upwelling radiance I_{ground} at the ground level is proportional to $f(\theta_s,\phi_s;\theta_r,\phi_r)$. This second assumption clearly is not valid for turbid atmospheres and for highly specular surfaces like water. Under these two assumptions we can replace $\rho(x,y)$ in eq (1) with $\pi f(\theta_s,\phi_s;\theta_r,\phi_r)$. Note that BRDF's for natural surfaces are usually asymmetric and cause the PSF to be asymmetric for all view directions, including nadir. The PSF for non-Lambertian surfaces is then given by :

$$PSF(x,y,\ldots) \;=\; \frac{\kappa_s\;\Delta l}{4\;\pi}\sum_{k=1}^{K}\frac{\tau(r_k)\;f(\theta_s,\phi_s;\theta_{r,k},\phi_{r,k})\cos\theta_{r,k}\;f(\theta_{p,k})\;dx\;dy}{r_k^2}\exp(-\kappa_t(K-k)\Delta l), \tag{3}$$

where $\phi_{r,k}$ is the view azimuth angle of surface dA from point $\vec{P_k}$.

4 Simulation of Scenes with Heterogeneous Surface Cover

The Earths, surface is composed of a mosaic of various surface types such as vegetation, bare soil and water, each with distinct BRDF's. To simulate an oblique view over a heterogeneous surface the following algorithm was used :

1. For each surface BRDF $f_i(\theta_s, \phi_s; \theta_r, \phi_r)$, $i = 1, 2, \ldots, N$ compute the point spread function $PSF_i(x, y, \ldots)$ using eq (3).
2. Generate a binary image $Q_i(x, y)$ for each surface type i, where $Q_i(x, y) = 1$ if the point (x, y) has surface cover type i and 0 otherwise.
3. Convolve each image $Q_i(x, y)$ with its point spread function $PSF_i(x, y, \ldots)$.

The measured radiance image is then given by :

$$I_{measured}(x, y) \;=\; \frac{E_0}{\pi}\tau_s \sum_{i=1}^{N}\Big[\tau_r Q_i(x_0, y_0) f_i(\theta_s, \phi_s; \theta_r, \phi_r) \;+\; Q_i(x, y) \otimes PSF_i(x, y, \ldots)\Big] \;+\; I_{path}. \quad (4)$$

Equation (4) shows that the adjacency blurring effect is the superposition of ground cover type images convolved with their corresponding point spread functions.

To illustrate the method on an example we used scattering phase function and BRDF's found in the literature.

To approximate a "hazy" atmosphere the Henyey-Greenstein phase function was used with the asymmetry factor $\Theta = 0.75$ (Liou (1980)). The Henyey-Greenstein phase function is defined as :

$$f(\theta_p) = \frac{1 - \Theta^2}{(1 + \Theta^2 - 2\Theta\cos\theta_p)^{3/2}}. \quad (5)$$

We selected a $\kappa_t = 0.8$, $\kappa_a = 0.05$ for an aerosol laden atmosphere of 1000 m height with 20 layers and a surface of 3000 m by 3000 m horizontal extent with 30 by 30 pixels.

The BRDF of bare ground was taken from Hapke (1981) :

$$f(\theta_s, \phi_s; \theta_r, \phi_r) \;=\; \frac{\omega}{4\pi}\frac{1}{\mu_s + \mu_r}\Big[\{1 + B(g)\}P(g) + H(\mu_s)H(\mu_r) - 1\Big], \quad (6)$$

where ω is the average single scattering albedo, $\mu_s = \cos\theta_s$, $\mu_r = \cos\theta_r$, $\cos g = \mu_s\mu_r + \sin\theta_s\ \sin\theta_r$ $\cos(\phi_r - \phi_s)$, $B(g) = B_0/[1 + h^{-1}\tan(g/2)]$, $B_0 = S(0)/(\omega P(0))$, $P(g) = 1 + b\cos g + c[(3\cos^2 g - 1)/2]$ and $H(x) = (1 + 2x)/(1 + 2[1 - \omega]^{1/2}\, x)$. The BRDF parameters chosen were : $\omega = 0.57$, $S(0) = 0.48$, $h = 0.21$, $b = 0.86$ and $c = 0.7$. The BRDF of vegetated surface was taken from a parametric model by Pinty et al (1990) with the same notation as above where not listed:

$$f(\theta_s, \phi_s; \theta_r, \phi_r) \;=\; \frac{\omega}{4\pi}\frac{\nu_s}{\nu_s\mu_s + \nu_r\mu_r}\Big[P_v(g)\ P(g) + H\Big(\frac{\mu_s}{\nu_s}\Big)H\Big(\frac{\mu_r}{\nu_r}\Big) - 1\Big], \quad (7)$$

where ν_s and ν_r describe the leaf orientation distribution for the illumination and observation angles which depend on a parameter χ_l with range: $(-0.4 < \chi_l < 0.6)$, $P(g)$ is the leaf scattering phase function which is the Henyey-Greenstein function in eq (5), the function $P_v(g)$ depends on the variable $G = [\tan^2\theta_s + \tan^2\theta_r - 2\tan\theta_s\tan\theta_r\cos(\phi_s - \phi_r)]^{1/2}$, the radius of sun flecks r in $[m]$ and Λ the leaf area density in $[m^2 m^{-3}]$. We selected the following canopy parameters : $\omega = 0.8$, $\Theta = -0.4$, $\Lambda = 0.01$, $r = 1.$, $\chi_l = 0.2$.

For the water surface we assumed the BRDF to be a Henyey-Greenstein phase function $f(\theta_s, \phi_s; \theta_r, \phi_r) = \rho_{water}P(g)$ with the forward peak aligned with the specular reflectance direction $(\theta_s, \phi_s + \pi)$ or $g = \cos^{-1}[\mu_s\mu_r + \sin\theta_s\sin\theta_r\cos(\phi_s - \phi_r - \pi)]$. We selected a reflectance ρ_{water} of 2.55 % and an asymmetry factor of $\Theta = 0.95$.

In Figure 2 we show the point spread functions for (a) bare soil, (b) vegetation and (c) water. Note that the PSF's are asymmetric and that the PSF for water has a ridge in the specular reflection direction (left side) of the sun which has a zenith angle of 30^0.

In Figure 3 we show a simulated scene containing some rectangular vegetated surfaces (light gray) surrounded by bare soil (dark gray) and a lake (black) in the middle. The simulated scene measures 3 km by 3 km and is viewed from the below with a zenith angle of 60^0. The sun light is incident from above with a zenith angle of 30^0. To make faint radiance changes more visible we show the histogram equalized radiance image. One can see the effect of the specular reflection of the sunlight into the atmosphere on the radiance in the field at the top of image (b). The edges of the fields closer to the observer appear darker than the edges away from the observer. Near the lower edge of the lake, the radiance decreases while it increases at the upper edge due to the increased scattering above the water surface.

5 Conclusions

The extended radiosity method has been used to compute point spread functions for a layered atmosphere above a heterogeneous ground cover. The adjacency blurring effect was simulated for a scene containing vegetated, bare soil and water surfaces.

References

[1] C.C. Borel, S.A.W. Gerstl, "Simulation of partially obscured scenes using the radiosity method", *SPIE Vol. 1486*, pp.271-277, April 1991.

[2] C.C. Borel, S.A.W. Gerstl, "Atmospheric corrections using the volume radiosity method", *Proc. Int. Geoscience and Remote Sensing Symposium*, May 26-29, 1992, Houston, Texas, 1992.

[3] D.J. Diner and J.V Martonchik, "Atmospheric transmittance from spacecraft using multiple view angle imagery", *Applied Optics*, 24:21, pp.3503-3511, 1985.

[4] B. Hapke, "Bidirectional reflectance spectroscopy: 1. theory", *J. Geophys. Res.*, Vol. 86, No. B4, pp. 3039-3054, April, 1981.

[5] Y.J. Kaufman, "Atmospheric effects on remote sensing of surface reflectance", *SPIE proceedings*, 475:20-33, 1984.

[6] K.-N. Liou, *An introduction to atmospheric radiation.* Academic Press, Orlando, FL, 1980.

[7] R. Richter, "A fast atmospheric correction algorithm applied to Landsat TM images", *Int. J. Remote Sensing*, 11, pp.159-166, 1990.

[8] D. Tanré, M. Herman and P.Y. Deschamps, "Influence of the background contribution upon space measurements of ground reflectance", *Applied Optics*, 20:20, pp.3676-3684, 1981.

[9] W.A. Pearce, "A study of the effects of the atmosphere on thematic mapper observations", *Report 004-77, EG&G*, Washington Anal. Serv. Center, Riverdale, MD, 1977.

[10] B. Pinty, M. Verstraete and R. Dickinson, "A physical model of the bidirectional reflectance of vegetation canopies: 2. inversion and validation.", *J. Geophys. Res.*, Vol.95, No. D8, pp.11767-11775, 1990.

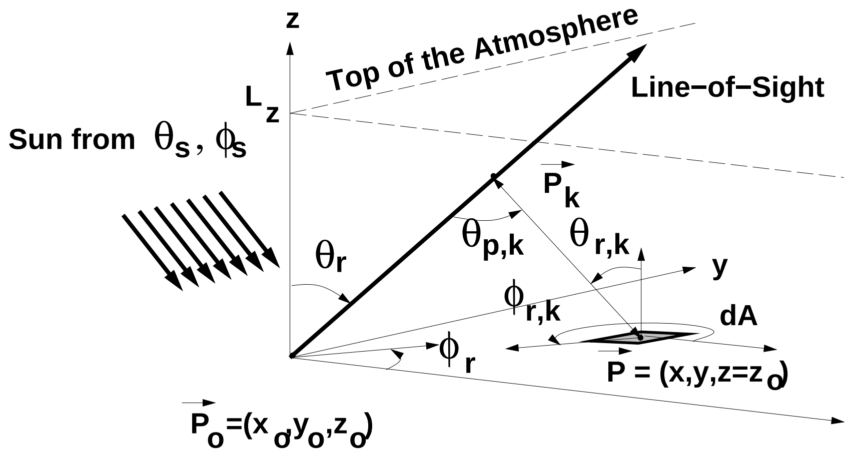

Figure 1 Geometry for computing the point spread function.

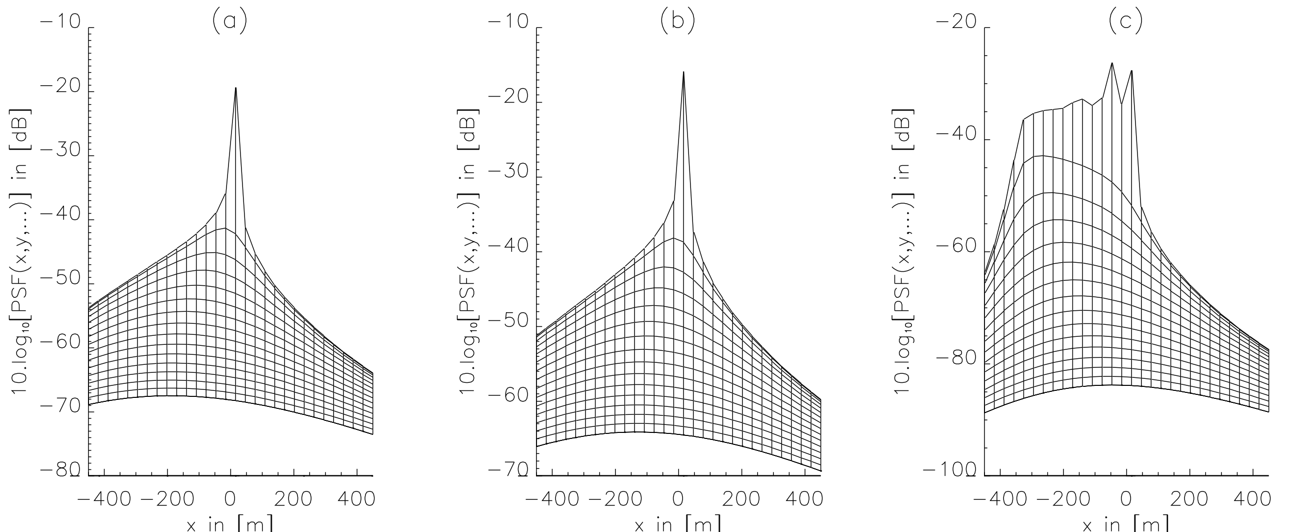

Figure 2 Point spread functions of (a) bare soil, (b) vegetation and (c) water with the z-axis in logarithmic scale and the y-axis points into the paper.

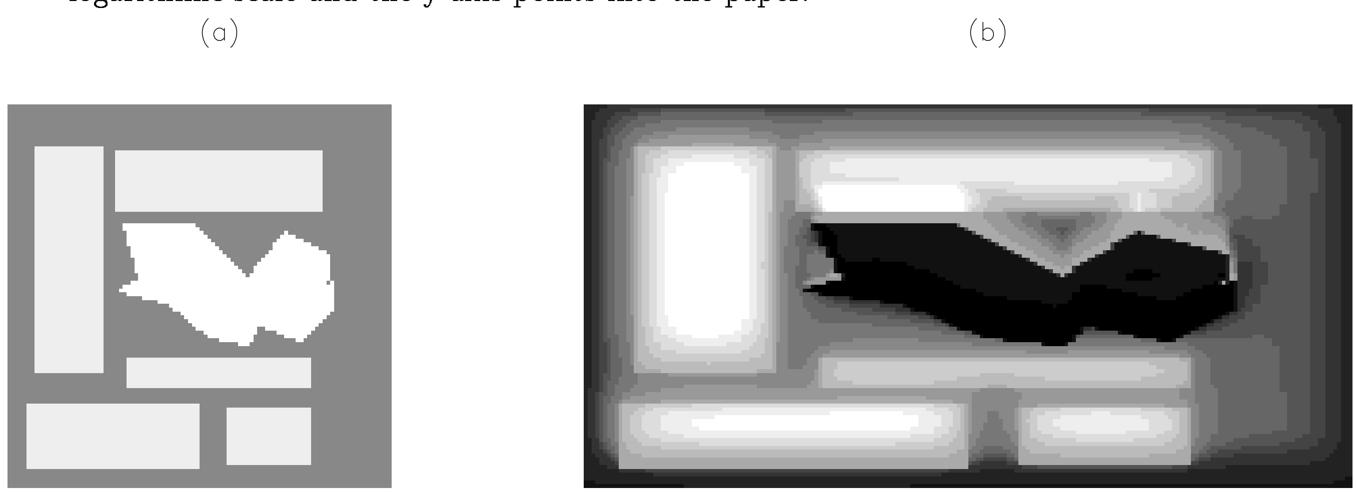

Figure 3 Simulated scene from (a) above and (b) viewed through atmosphere from the below at 60^0 view zenith angle and illuminated from above at 30^0 sun zenith angle.